Translational multiple sclerosis research in primates

Dunham, Jordon Tyler-Nathan

Blockade of CD127 exerts a dichotomous clinical effect in marmoset experimental autoimmune encephalomyelitis

Jordon Dunham[1,2,3,4], Li-Fen Lee[5], Nikki van Driel[1], Jon D. Laman[4], Irene Ni[6], Wenwu Zhai[6], Guang-Huan Tu[5], John C. Lin[5], Jan Bauer[7], Bert A. 't Hart[1,2,3,4], and Yolanda S. Kap[1,2]

[1]Dept. of Immunobiology, Biomedical Primate Research Centre, Rijswijk, The Netherlands;
[2]MS Centre Erasmus, Rotterdam, The Netherlands;
[3]Dept. of Immunology, Erasmus MC, University Medical Center, Rotterdam, The Netherlands;
[4]University Groningen, University Medical Center, Dept. of Neuroscience, Groningen, The Netherlands;
[5]Dept. of Experimental Medicine, Rinat, Pfizer Inc, South San Francisco, CA;
[6]Dept. of Protein Engineering, Rinat, Pfizer Inc, South San Francisco, CA;
[7]Medical University of Vienna, Center for Brain Research, Vienna, Austria.

Abstract

Non-human primate models of human disease have an important role in the translation of a new scientific finding in lower species into an effective treatment. In this study, we tested a new therapeutic antibody against the IL-7 receptor α chain (CD127), which in a C57BL/6 mouse model of experimental autoimmune encephalomyelitis (EAE) ameliorates disease, demonstrating an important pathogenic function of IL-7. We observed that while the treatment was effective in 100% of the mice, it was only partially effective in the EAE model in common marmosets (*Callithrix jacchus*), a small-bodied Neotropical primate. EAE was induced in seven female marmoset twins and treatment with the anti-CD127 mAb or PBS as control was started 21 days after immunization followed by weekly intravenous administration. The anti-CD127 mAb caused functional blockade of IL-7 signaling through its receptor as shown by reduced phosphorylation of STAT5 in lymphocytes upon stimulation with IL-7. Group-wise analysis showed no significant effects on the clinical course and neuropathology. However, paired twin analysis revealed a delayed disease onset in three twins, which were high responders to the immunization. In addition, we observed markedly opposite effects of the antibody on pathological changes in the spinal cord in high versus low responder twins. In conclusion, promising clinical effect of CD127 blockade observed in a standard inbred/SPF mouse EAE model could only be partially replicated in an outbred/non-SPF non-human primate EAE model. Only in high responders to the immunization we found a positive response to the treatment. The mechanism underpinning this dichotomous response will be discussed.

Introduction

IL-7 is a type 1 cytokine family member that plays a crucial role in both lymphopoiesis and homeostasis of B and T lymphocytes [1]. The IL-7 signaling pathway has raised much interest as target of immunotherapy in human autoimmune disease. Recent findings showed that blockade or deletion of the IL-7 receptor ameliorates T-cell-mediated autoimmune disease, such as in C57BL/6 and SJL/J mice models of experimental autoimmune encephalomyelitis (EAE); the animal model for MS [2-4].

Signaling is mediated through binding of IL-7 to a heterodimeric receptor composed of a common γ chain (CD132) shared between several cytokine receptors, paired with an IL-7 receptor-specific α chain (IL-7Rα/CD127) [5]. Under normal circumstances, engagement of the IL-7R by IL-7 on naive and memory T cells exerts anti-apoptotic effects, resulting in increased cell survival [5]. Whereas IL-7R is typically down-regulated on T cells after activation, it is selectively up-regulated on populations destined to develop into memory T cells [6]. IL-7 has also been shown to drive the expansion of high avidity, myelin-specific $CD4^+$ T cells isolated from peripheral blood mononuclear cells (PBMC) from multiple sclerosis (MS) patients [7] and elevated plasma levels of IL-7 are associated with disease severity in systemic juvenile rheumatoid arthritis patients [7,8]. A direct relationship between IL-7 and psoriasis has been found [9]. Collectively these data highlight the IL-7 signaling pathway as an attractive therapy target in autoinflammatory disease.

The aim of the current study was to test whether the promising and robust clinical effects observed in the inbred/specific-pathogen free (SPF) mouse EAE models, could be replicated in an outbred, non-SPF model more closely related to humans. We used a well-established EAE model in the common marmoset (*Callithrix jacchus*). EAE was induced by immunization with peptide 34-56 of human myelin oligodendrocyte glycoprotein (MOG34-56) in incomplete Freund's adjuvant (IFA) [10]. Previous findings hint at a role for the IL-7 signaling pathway in EAE developing in marmosets immunized with recombinant human myelin oligodendrocyte glycoprotein (rhMOG)/CFA. Depletion of $CD20^+$ B cells in the marmoset EAE model inhibits the activation and lymph node emigration of T cells and consequently prevents the development of clinical symptoms and pathology [11-13]. In B-cell depleted marmosets, CD127 expression on T cells was not down-regulated, but IL-7 mRNA levels were profoundly suppressed [12]. In addition, in B-cell depleted marmosets the viral load of CalHV3, which is the marmoset lymphocryptovirus equivalent of Epstein-Barr virus (EBV), was reduced [14]. The human EBV^+ B cell constitutively secretes IL-7 [15], suggesting that the $CalHV3^+$ B cell is one of the IL-7 sources in the marmoset EAE model.

The experiment comprised seven marmoset twins. Fraternal siblings were treated with a chimeric mAb raised against human CD127 blocking IL-7 mediated signaling in marmoset mononuclear cells, or PBS as control. The weekly treatment was started 21 days after immunization, well after priming and clonal expansion of autoreactive T and B cells. Here, we report that contrary to a profound clinical effect on EAE of CD127 blocking observed in inbred, SPF mice, blockade of CD127 in the outbred conventionally housed marmoset did not exert a general beneficial effect on the clinical course of EAE. Examination of a possible effect in individual twins, we observed a delayed EAE onset in three twins, which similar to the C57BL/6 mouse strain were high responders to sensitization against MOG.

In conclusion, the data obtained in the marmoset EAE model only partially replicate the robust clinical effect of anti-CD127 mAb in mouse EAE and predict that only a subset of patients will show a clinical response against the treatment.

Material and Methods

Animals

Seven adult (female, age ranging between 2-5 years) outbred common marmoset twins were obtained from the purpose-bred colony at the Biomedical Primate Research Centre (Rijswijk, Netherlands).

Fraternal twin siblings were equally and randomly divided over two groups such that the two experimental groups each contained one sibling of each twin. The placebo-treated group had an average (± SD) body weight of 421±50 gram and the anti-CD127 mAb-treated group had an average body weight of 394±42 gram. The groups had an average age of 42±10 months. All experimental procedures were reviewed and approved by the Institute's Animal Ethics Committee and animals were housed and handled according to the Dutch Law on animal experimentation. The animal facilities of BPRC have been inspected and accredited by the Association for Assessment and Accreditation of Laboratory Animal Care International (AAALAC) in full.

EAE induction

EAE was induced with a synthetic peptide representing amino acids 34-56 of human MOG (MOG34-56; Peptide 2.0 Inc, Chantilly, VA) emulsified in IFA (Difco Labs, Detroit, MI). The inoculum contained 100 µg MOG34-56 in 200 µl PBS and was emulsified in 200 µl IFA by gentle stirring for at least 1 h at 4ºC. The emulsion was injected as 4 spots of 100 µl into the dorsal skin under sedation by alfaxalone (10 mg/kg alfaxan; Vetoquinol, Den Bosch, The Netherlands) with booster immunizations occurring every 28 days until development of overt neurological disease (EAE score $\geq$ 2) was observed. Marmosets were monitored and scored daily based upon a standard scoring system [16]. Briefly, score 2= ataxia or optic disease; and 2.5= paresis of two limbs. For ethical reasons monkeys were sacrificed once paresis of two or more limbs (score ≥ 2.5) was observed.

Anti-CD127 mAb administration

The test substance (21D8) was a chimeric mAb raised against marmoset CD127. The chimeric Ab was generated by fusing the VH and Vk gene of mAb 21D8 with that of human IgG1 constant region and of the k chain constant region, respectively. This recombinant anti-CD127 mAb was produced by Pfizer Inc. (San Francisco, CA) and injected intravenously such that animals received 10 mg/ml/kg per treatment. Fraternal control siblings were administered 1 ml PBS/kg body weight. Dosing was performed once a week starting at 21 days after immunization and continued for 14 weeks.

Blood and tissue collection

Marmosets reaching EAE score 2.5 were sedated by intramuscular injection of alfaxalone for collection of venous blood volume of 1.5 ml. Marmosets were subsequently euthanized by infusion of sodium pentobarbital (Euthesate®; Apharmo, Duiven, The Netherlands). Upon necropsy, lymph nodes from axillary (ALN), inguinal (ILN), lumbar (LLN) and cervical (CLN) regions as well as the spleen were harvested. The brain, spinal cord, and optic nerve were collected for histology (formalin) and immunohistochemistry (snap frozen in liquid nitrogen).

Venous blood was collected from the femoral vein into EDTA-vacutainers every other week during the course of the study and at necropsy. PBMC from blood and mononuclear cells (MNC) from secondary lymphoid organs (SLO) were isolated as previously described [17].

Proliferation assay

MNC isolated from peripheral blood or SLO were tested for proliferation against MOG34-56 (5 µg/ml), rhMOG (5 µg/ml), ovalbumin (Ova; 5 µg/ml), and ConA (5 µg/ml) as described previously [17]. Incorporation of ^{3}H-Thymidine (0.5 µCi/well). was determined using a matrix 9600 β-counter (Packard 9600; Packard Instrument Company, CT). Results are expressed as stimulation index, which is calculated by dividing the counts per minute (cpm) of stimulated cells by the cpm of unstimulated cells. A stimulation index above 2 is set as cut-off for a positive proliferative response.

Cellular phenotyping

PBMC and MNC from SLO were phenotyped by flow cytometry [17]. Briefly, cells were stained with a violet viability stain (Invitrogen, Molecular Probes, Carlsbad, CA) to exclude dead cells followed by an FcR blocking reagent (Miltenyi Biotec). Subsequently, cells were stained with commercially available mAb against CD3 (SP43-2), CD4 (L200), CD27 (MT721), CD45RA (5H9), CD56 (NCAM 16.2), and HLA-DR (L243) (All from BD Biosciences, San Diego, CA); CD279 (J105) and CD127 (ebioDR5) (both from Ebiosciences, San Diego, CA); CCR7 (150503, R&D systems, Minneapolis, MN); CD20 (H299, Beckman Coulter. Pasedena, CA); CD40 (B-B20, Abcam, Cambridge, UK), and CD8 (LT-8, Serotec, Dusseldorf, Germany). Cells were fixed in 1% Cytofix (BD Biosciences).

Flow cytometric measurements were performed utilizing the FACS LSRII and data was analyzed with FlowJo software (Treestar, Ashland, OR). The gating strategy to determine phenotype was as follows: live cells were first selected as violet viability stain negative cells. Next, lymphocytes were identified based on forward scatter (FSC) and side scatter (SSC). Within the live lymphocyte population, $CD3^{-}$ and $CD3^{+}$ cells were determined. Within the $CD3^{+}$ T cell population, $CD4^{+}CD8^{-}$ and $CD4^{-}CD8^{+}$ cells were distinguished. Within these subpopulations, other markers, such as CCR7 and PD1, were analyzed. The figures show the percentage of cells within the parent gate, which is indicated before the forward slash (/).

In vitro phosphorylation of STAT5 as bioassay for IL-7 signaling

Phosphorylation of STAT5 (pSTAT5) was measured in PBMC and MNC obtained from SLO. Briefly, $2x10^{5}$ cells were stimulated with 1 ng/ml recombinant human IL-7 (rIL-7, Peprotech, Rocky Hill, NJ) for 15 min at 37°C. Cells were fixed with 1% Cytofix (BD Biosciences) and

permeabilized with 100% methanol (VWR, Amsterdam, The Netherlands) for 10 min at 4°C. After washing, cells were stained with mAb directed against pSTAT5, CD3 and CD4 (BD Biosciences). Flow cytometric measurements were performed utilizing the FACS LSRII (BD Biosciences) and data were analyzed with FlowJo software (Treestar). Lymphocytes were identified based on forward scatter (FSC) and side scatter (SSC). Within the lymphocyte population, $CD3^+$ cells were determined, which were subsequently divided into $CD4^-$ and $CD4^+$ cells. An Ab against CD8 could not be included due to limited availability of fluorochromes resistant to methanol. Within the $CD4^-$ and $CD4^+$ populations, cells positive for pSTAT5 were selected.

Quantitative PCR

The isolation of RNA and the qPCR assay were performed as described previously [17]. Briefly, isolation of RNA from snap frozen spleen and lymph nodes was performed using an RNeasy minikit following manufacturer's protocol (Qiagen, Hilden, Germany). cDNA was synthesized from mRNA using the RevertAid First Strand cDNA Synthesis Kit (Fermentas, St. Leon-Rot, Germany) and qPCR was performed using an iTaq supermix and CFX96 Real-Time system (Bio-Rad, Hercules, CA). Transcript levels were normalized against the reference gene Abelson (ABL) [18].

Immunohistochemistry and histology

Immunohistochemical staining was performed on paraffin embedded tissue isolated at necropsy. Paraffin sections were cut into 3-5 mm, deparaffinized and stained with haematoxylin/Eosin and Luxol Fast Blue/Periodic Acid Schiff to assess inflammation and demyelination. Tissue sections were also stained with anti-CD3 for T cells (A0452; Dako), anti-MRP14 for macrophages (BMA Biomedicals, Switzerland), anti-CD20 for B cells (clone L26; Thermo Scientific) and an Ab against proteolipid protein (PLP, MCA 839G; Serotec,UK).

Inflammation was visualized by staining infiltrating cells with hematoxylin and eosin, CD3, CD20, or MRP14. The inflammatory index of the spinal cord is given as the average number of inflamed blood vessels/spinal cord cross section. A total of 10-12 sections per animal were analyzed. WM demyelination in the spinal cord was measured on a total of 10-12 cross sections by using a morphometric grid. Demyelination in the brain was determined as follows: brain sections stained for LFB/PAS were scanned at 1000 dpi with an Agfa Duoscan scanning device. Images were then imported in the public domain program ImageJ (version 1.46r). In density slice mode, first the total amount of white matter was measured. Lesions in WM were selected by freehand mode and their size was measured. Finally the demyelination in WM was calculated as percentage of total WM. Six sections of the brain of each animal were analysed, amounting to approximately 6 cm^2 of WM in total.

Statistics

Clinical data are presented as survival curves (Kaplan-Meier estimator). Difference in (disease-free) survival was statistically tested using the Log-Rank test. Grouped data are presented as box and whisker plots with the box extending from the 25th and 75th percentiles, the whiskers extending from min to max, and the median data point being shown as a line. Individual data is presented as dot plots, with bars indicating mean values. Statistical analysis was performed using Prism 6.0b for Mac OS X. Data was analyzed using the Mann-Whitney U test. $p<0.05$ was considered statistically significant.

Results

Functional blockade of CD127

Functional blockade of marmoset CD127 by the anti-CD127 mAb was analyzed on biweekly-collected PBMC and on MNC isolated from SLO taken at necropsy. Cells were stained with a commercially available fluorochrome-labeled anti-human CD127 mAb (anti-CD127-FITC; ebioDR5). *In vitro* tests showed that this labeled detection Ab binds to an overlapping epitope as the therapeutic anti-CD127 mAb (data not shown). Therefore, a reduction of CD127$^+$ cells shows that CD127 is occupied by the therapeutic anti-CD127 mAb or that CD127$^+$ cells are deleted.

Figure 1A shows clearly reduced binding of anti-CD127-FITC mAb to CD4$^+$ and CD8$^+$ T cells in PBMC collected at 1, 3 and 5 weeks after first administration (on psd 21) of the therapeutic (anti-CD127) mAb. However, the level of anti-CD127-FITC binding increased progressively in the Ab treated group and the difference between treated and control groups became negligible beyond day 70, indicating decreasing occupancy of CD127 by the administered therapeutic mAb. The reduction was equally strong in the CD4+ and CD8+ T-cell compartments. Nevertheless, at necropsy a significantly lower percentage of anti-CD127-FITC mAb binding to CD4$^+$ and CD8$^+$ MNC from blood, spleen, and ALN was detected (**Figure 1B**), suggesting that the test substance was still biologically active. CD127 blockade did not induce a compensatory mechanism of enhanced IL-7 or CD127 mRNA expression.

To assess whether *in vivo* blockade of CD127 by the therapeutic mAb abrogated IL-7 signaling, the phosphorylation of STAT5 was analyzed after *ex vivo* exposure of MNC to IL-7. MNC from venous blood or SLO were stimulated with 1 ng/ml IL-7 for 15 min and subsequently stained for pSTAT5. The percentages of pSTAT5$^+$ T cells following first administration of the therapeutic mAb were significantly reduced (**Figure 2A**), correlating with the significantly reduced binding of anti-CD127-FITC mAb. The percentage of cells positive for pSTAT5 was also reduced in MNC from SLO, although inhibition was not significantly different between control and treated animals (**Figure 2B**).

In conclusion, the therapeutic anti-CD127 mAb displayed significant *in vivo* target cell binding as well as biological activity in the marmoset EAE model. Although the effect is detectable in the blood for a limited period of time, it could still be detected in the lymphoid tissue compartment analyzed at necropsy.

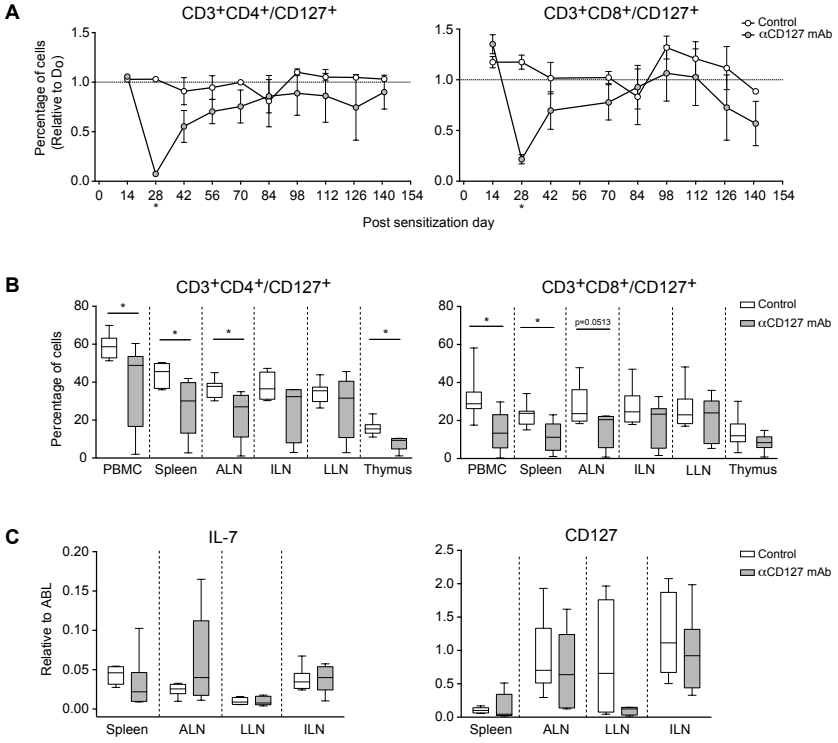

Figure 1. The anti-CD127 mAb blocks CD127 on T cells in the periphery and secondary lymphoid organs. Paired marmoset siblings received weekly intravenous injection of anti-CD127 mAb or placebo. PBMC were isolated every two weeks and MNC from secondary lymphoid organs were obtained at necropsy. CD127 blockade was analyzed by flow cytometry. **A,** The percentage of $CD127^+$ cells in PBMC relative to day 0, i.e. 21 days before treatment. Shown is mean ± SEM of the 7 animals per group. The x-axis represents the post sensitization day. Note that during the disease course, the number of animals in the group averages decreases due to ethical withdrawal from study. **B,** The percentage of $CD127^+$ cells within the $CD3^+CD4^+$ and $CD3^+CD8^+$ T cells isolated from blood and secondary lymphoid organs harvested at necropsy. Each Box-Whisker plot represents 7 animals. **C,** IL-7 and CD127 mRNA expression levels were determined by qPCR. Shown is the expression relative to the reference gene ABL. The number of animals included per organ differed due to availability of material: PBS-treated marmosets: spleen n=6, ALN n=7, ILN n= 5, LLN n=4; Anti-CD127 mAb treated marmosets: spleen n=5, ALN n=5, LLN n=5, ILN n=6. Statistical significance ($P<0.05$) is indicated by an asterisk.

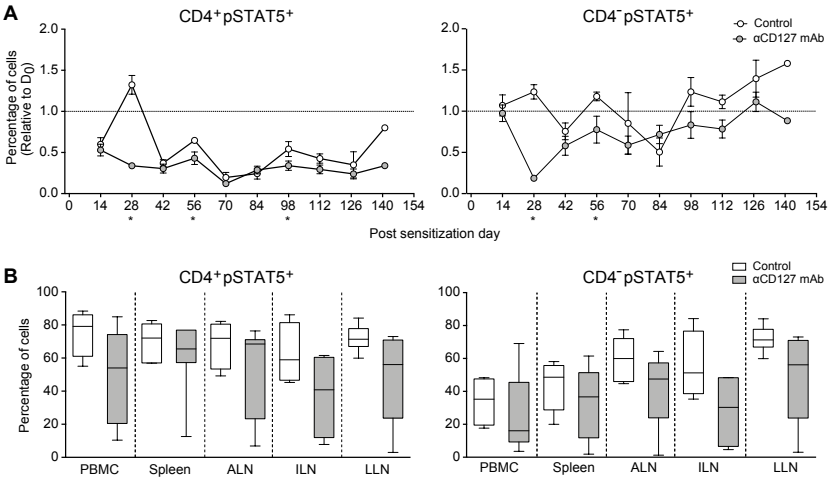

Figure 2. Inhibition of STAT5 phosphorylation by anti-CD127 mAb. PBMC were isolated every two weeks and MNC from secondary lymphoid organs were obtained at necropsy. Cells were stimulated with 1 ng/ml recombinant IL-7 for 15 min and stained for pSTAT5. The percentage of pSTAT5$^+$ cells was analyzed by flow cytometry for CD3$^+$CD4$^+$ and CD3$^+$CD4$^-$ cells. **A,** The percentages of pSTAT5$^+$ cells within the CD4$^+$ or CD4$^-$ T cell populations during the EAE course relative to day 0 are shown. The x-axis represents the post sensitization day. Shown is mean ± SEM for 7 marmosets per group. Note that during the disease course the number of animals in the group averages decreases. **B,** Shown are the percentages (y-axis) of pSTAT5$^+$ cells within the CD4$^+$ or CD4$^-$ T cell compartment of MNC obtained at necropsy. Statistical significance ($P<0.05$) is indicated by an asterisk.

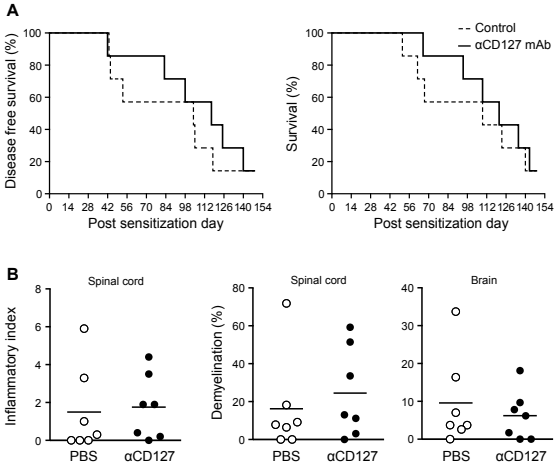

Figure 3. Blockade of CD127 delayed the day of onset of clinical symptoms in three of the six twins. Marmosets were euthanized once they reached a score 2.5, or at a predetermined study end date (psd 150). **A,** Disease free survival (left graph) is survival until clinical score 2 and survival (right graph) is survival until day of sacrifice with EAE. No significant differences were observed according to the Log-Rank test, showing that treatment had no impact on the onset of disease ($P=0.58$) or on total survival ($P=0.67$). **B,** the inflammatory index of the spinal cord is given as the average number of inflamed blood vessels/spinal cord cross section. Demyelination in the white matter is shown as a percentage. No significant differences were observed between control and treated animals.

Weekly administration of anti-CD127 mAb did not result in general protection against EAE

Marmosets immunized with MOG34-56/IFA were assessed daily for clinical signs of EAE (**Supplemental figure 1**). Marmosets were humanely sacrificed upon reaching EAE score 2.5, or at a predetermined end date (psd 150). The survival curves in **figure 3** show a modest delay in the onset of neurological deficits in the group receiving the anti-CD127 mAb, although the effect was not statistically significant. In one set of twin siblings (M10033/10034) we did not observe signs of neurological deficit; therefore, they were withdrawn from the experiment alive and excluded from further postmortem immunological analysis.

Inflammation and demyelination in the central nervous system (CNS) are pathological hallmarks of EAE. No significant differences were observed between treated and control animals with respect to inflammation and demyelination when analyzed as complete groups (**Figure 3B**).

In conclusion, no significant effect of the anti-CD127 mAb on the clinical course and pathology was observed in the marmoset EAE model.

Blockade of CD127 did not have a general effect on T-cell survival and expression of activation markers

Hematological parameters were assessed during the course of the study. No treatment-related alterations in the percentages of monocytes, neutrophils and lymphocytes were observed (**Supplemental figure 2**). Flow cytometric analysis revealed no change in the percentage of total $CD3^+$ T cells, $CD4^+$ T cells or $CD8^+$ T cells, neither in PBMC nor in the SLO (**Supplemental figure 2**). In addition, no alterations were observed in the percentage of T cells expressing CD56, a marker for NK-CTL, or CD45RA, a marker that can be used to distinguish naïve and memory T cells (data not shown).

A detailed immune phenotyping for activation and identification markers was performed during the course of the study and at necropsy. Blockade of CD127 had a significant effect on the percentage of $CCR7^+$ T cells in PBMC at necropsy (**Figure 4A**), which was not observed in biweekly bleedings (data not shown). This effect was seen both in $CD4^+$ and $CD8^+$ T cells regardless of CD45RA expression (data not shown). Despite an apparent trend toward reduced PD1 expression on $CD8^+$ T cells isolated from the ALN at necropsy, no statistically significant treatment effects in PD1 expression in both $CD4^+$ and $CD8^+$ T cells during biweekly bleedings or at necropsy were observed (**Figure 4B**).

In addition, we observed different CD27 expression in $CD4^+$ PBMC at psd 42 and 112 (**Figure 4C**). However, at necropsy no difference in the $CD4^+$ subset was observed (data not shown). These findings are compatible with immunological changes associated with EAE onset, which are abrogated by the treatment with anti-CD127 mAb.

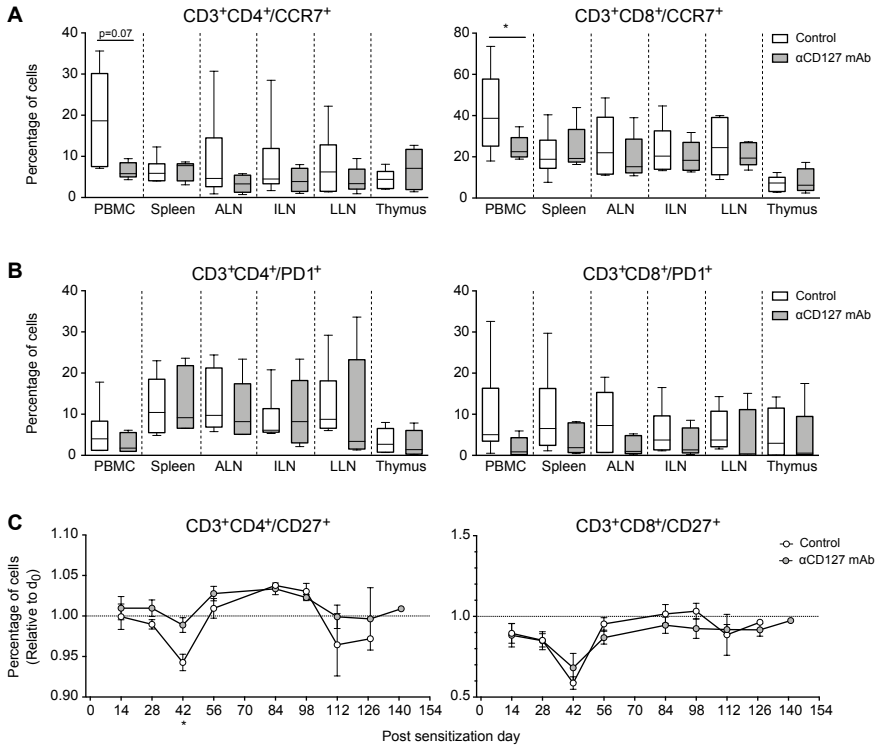

Figure 4. Frequencies of CCR7, CD27 and PD1 expressing cells are changed after CD127 blockade. CD127 blockade alters CCR7, CD27 and PD1 expression. CCR7, CD27 and PD1 expression was analyzed by flow cytometry. Cells were first gated on live lymphocytes, followed by $CD3^+$ cells that were subsequently divided into $CD4^+CD8^-$ or $CD4^-CD8^+$ cells **A,** percentage of $CCR7^+$ cells within the $CD3^+CD4^+$ and $CD3^+CD8^+$ T cells isolated from blood and secondary lymphoid organs harvested from control (n=6) and treatment marmosets (n=5) at necropsy. **B,** Percentages of PD1 $(CD279)^+$ cells within $CD3^+CD4^+$ or $CD3^+CD8^+$ isolated from blood and secondary lymphoid organs from control (n=6) and treatment marmosets (n=5) harvested at necropsy. **C,** Percentage of $CD27^+$ cells within $CD3^+CD4^+$ and $CD3^+CD8^+$ T cells isolated from peripheral blood (n=6) at biweekly bleedings. Statistical significance ($P<0.05$) is indicated by an asterisk.

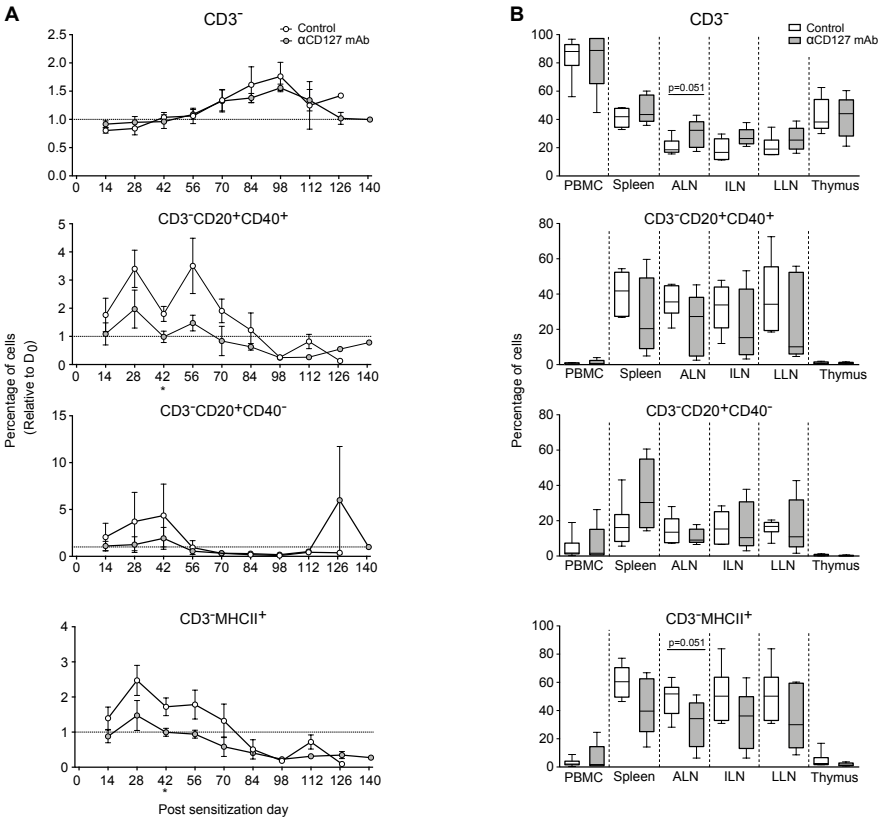

Figure 5. Alterations in B cells after CD127 blockade. PBMC (n=6) isolated every two weeks (**A**) and isolated MNC were obtained from treatment (n=5) and control (n=6) marmosets at necropsy (**B**) were stained for CD3, MHC Class II, the B cell marker CD20, and the co-stimulatory molecule CD40. Represented are cells within the live lymphocyte population. Statistical significance (P<0.05) is indicated by an asterisk.

Prior studies with anti-CD20 mAb in the EAE model induced with MOG34-56/IFA, highlighted an important pathogenic role of $CD20^+CD40^+$ B cells [13,14]. Hence, the effect of the anti-CD127 mAb was tested on this B cell subset. **Figure 5A** shows that following immunization with MOG34-56/IFA increased percentages of $CD3^-CD20^+$ $CD40^+$ MNC, as well as $CD3^-$ and MHCII-DR^+ MNC were found in PBMC during biweekly bleedings. This increase was less pronounced in the treatment group (**Figure 5A**). In the lymphoid organs collected at necropsy, there was a trend towards a reduced percentage of $CD3^-CD20^+CD40^+$ and $CD3^-$MHCII-DR^+ cells in spleen, ALN and ILN and an increased percentage of $CD3^-CD20^+CD40^-$ cells in the spleen of anti-CD127 mAb treated monkeys (**Figure 5B**). However, the effect was not statistically significant.

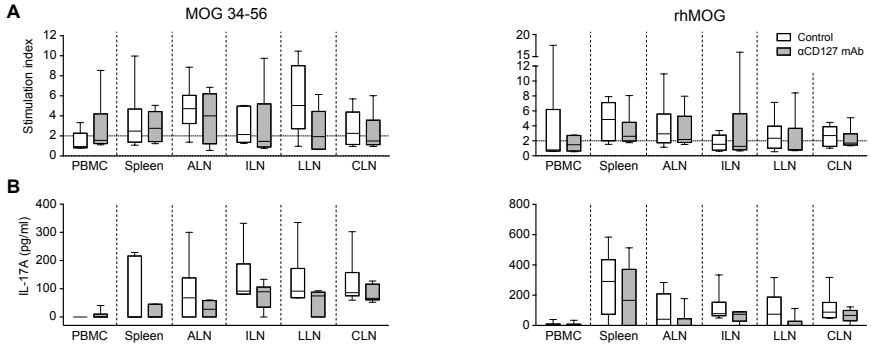

Figure 6. CD127 blockade does not affect proliferation or IL-17A production. A, MNC (n=6) isolated at necropsy were stimulated with MOG34-56 or rhMOG for 48 h and radiolabeled with ^{3}H-thymidine. The stimulation index is calculated by dividing the counts per minute (cpm) of stimulated cells by the cpm of non-stimulated cells. A stimulation index above 2 is considered as proliferation. **A,** No significant differences in proliferation were observed between treatment and control animals after ex vivo stimulation by MOG34-56 or rhMOG. **B,** Supernatants were analyzed for the production of IL-17A following 48h stimulation. No significant differences in IL-17A production were found between treatment and control animals after ex vivo stimulation by MOG34-56 or rhMOG. Statistical significance ($p<0.05$) is indicated by an asterisk.

Blockade of CD127 did not alter T cells responses to antigen-stimulation

We investigated whether treatment with the anti-CD127 mAb altered the proliferative response of T cells to *ex vivo* stimulation with MOG34-56 or rhMOG. Blockade of CD127 did not significantly alter the proliferative response to MOG34-56 or rhMOG, neither in PBMC collected during the disease course (data not shown), nor in MNC from lymphoid organs collected at necropsy (**Figure 6A**).

Next, the production of a panel of cytokines after *ex vivo* stimulation with MOG34-56 and rhMOG was analyzed. The levels of IFN-γ and IL-2 in supernatants from MOG34-56 and rhMOG stimulated MNC were negligible (data not shown). Although IL-17A was detected after stimulation, no difference between the treatment group and control group was observed (**Figure 6B**). Furthermore, no significant differences between groups were observed for mRNA expression levels of TNF-α, TGF-β1, IL-10, Foxp3, M-CSF and GM-CSF in total spleen or LN (data not shown).

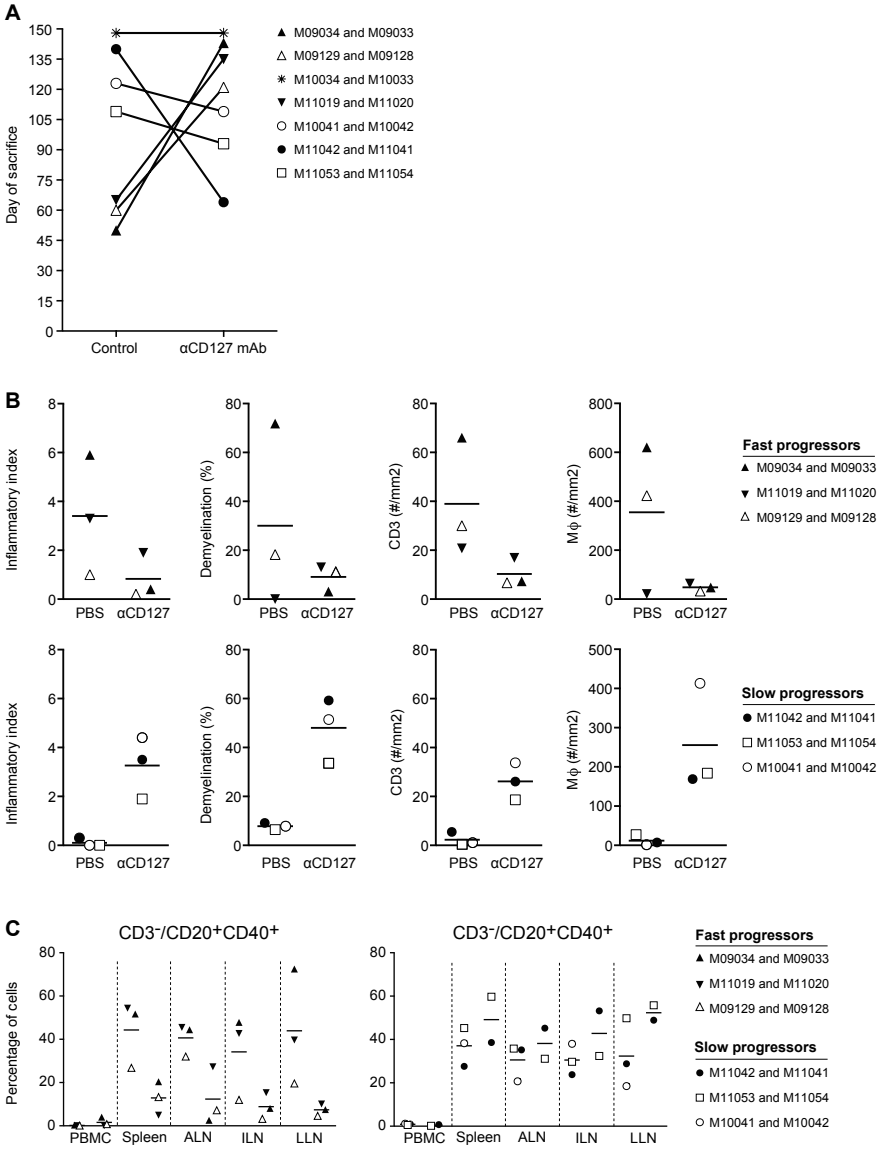

Figure 7. Distinct immunological differences between fast and slow EAE progressors. Data was further analyzed by subgrouping twins according to the response to treatment. **A**, Paired analysis of twin marmosets at day of sacrifice with full-blown EAE. **B,** Inflammation, demyelination, and the number of infiltrated T cells and macrophages were reduced in the spinal cord of treated animals of fast progressor twins, but not in slow progressor twins. **C,** MNC were obtained at necropsy and stained for identification markers. The percentage of $CD20^{+}CD40^{+}$ cells within the $CD3^{-}$ lymphocytes isolated from secondary lymphoid organs harvested at necropsy. The phenotype of MNC cells of M10042 could not be measured due to technical failure.

Discussion

We report that promising clinical effects of CD127 (IL-7Rα) blockade in mouse EAE models were only partly replicated in the marmoset EAE model induced by immunization with MOG34-56 emulsified in IFA. While treatment with anti-CD127 mAb exerted a robust clinical effect in a genetically inbred mouse EAE model, responses to CD127 blockade were less obvious in the marmoset EAE model. One explanation for the different clinical effect of CD127 blockade might be that EAE in mice and marmosets are driven by different pathogenic mechanisms [19]. Another explanation may be the short period that functional blockade of IL-7 signaling was detectable in blood. However, we noticed that occupancy and blockade of CD127 by the therapeutic Ab could still be detected in T cells isolated from blood and SLO harvested at necropsy, which was often three to four days after the last dose. In contrast, the biweekly analysis of CD127 blockade in PBMC was seven days after the previous dose. This suggests, in scope of treatment frequency, that anti-drug antibody development had negligible impact on study outcome.

One surprising finding was the relatively limited impact of CD127 blockade on T-cell subsets and responses. Administration of recombinant IL-7 protein to EAE mice exacerbates disease while conversely treatment either therapeutically or prophylactically with anti-IL-7Rα neutralizing mAb mitigates EAE severity via partial depletion of naïve and effector memory CD4 and CD8 T cell subsets [2-4]. Although deficiencies in IL-7R alter both Th1 and Th17 populations, work by Lee et al. strongly supports the notion that IL-7 plays a role in the development of pathogenic Th1 cells, but not the Th17 cell [2]. These authors demonstrate that elevated levels of serum IL-7 predict Th1 driven forms of MS. In addition, murine and human naïve T cells differentiate into Th1 cells when stimulated with IL-7 [2]. Furthermore, anti-CD127 antibodies mitigate murine EAE severity at the expense of Th1 responses [2,3]. Although we cannot draw conclusions regarding IL-7 in Th1 responses in our model due to limited detection of IFN-γ in our model, we do show that CD127 blockade had negligible impact on IL-17A production, regardless of EAE progression.

An important characteristic of the outbred marmoset EAE model is heterogeneity in clinical and pathological presentation, which likely reflects genetic differences between individual monkeys. An interesting observation was an apparent treatment effect in a subgroup of marmosets, which were all characterized by fast disease progression. In previous experiments in which twins were used and the therapy failed, we observed that in most twins EAE develops around the same day (own unpublished observations). The present study consisted of 7 bone marrow chimeric twins where one sibling was treated with anti-CD127 mAb and one sibling with PBS. When comparing the day of sacrifice with full-blown EAE between siblings, we observed that in three twins (M09033/M09034, M09128/M09129, M11019/M11020; **Figure 7A**) the treated animals developed evident neurological impairment 60-90 days later than their PBS-treated siblings. These three PBS treated siblings developed EAE by day 55 and therefore these twins are called fast EAE progressors. In the other three twins that developed EAE at a much later stage and were therefore slow EAE progressors, no delay was observed in the treated sibling. In addition, typical EAE-related histological changes in the spinal cord histology were also reduced in the treated sibling of the fast progressor twins (**Figure 7B**). This may indicate that the anti-CD127 mAb blocked a pathogenic process that drives fast disease progression. Interestingly, we did observe a lower frequency of $CD3^{-}CD20^{+}CD40^{+}$ cells in spleen and lymph nodes of the anti-

CD127 mAb treated siblings of the fast EAE progressor twins compared to the PBS treated siblings (**Figure 7C**). Unfortunately the power analysis performed prior to start of this study, as an ethical requirement to limit the number of NHP used for research, did not account for such heterogeneous responses to CD127 blockade and thus precludes a post hoc analysis. We believe that this heterogeneity in response to CD127 blockade highlights challenges in the translation of data obtained in genetically inbred models to outbred populations, and may have implications on future trial design in MS studies.

The IL-7/CD127 pathway likely plays a role in MS pathogenesis. Polymorphisms of the IL7Rα gene are among the established non-HLA related immune genetic risk factors for MS [20]. Enhanced expression of both IL-7 protein and IL-7 mRNA is found in the cerebrospinal fluid of MS patients, with T cells isolated from the periphery and CNS exhibiting increased IL-7R expression [20,21]. Evidence now suggests that IL-7 promotes cytotoxicity of the CD8+ T cell in the MS patient, something not seen in healthy cohorts or animal models [7,21]. Unlike previous reports of a role in IL-7 in expansion of MBP specific T cells in MS patients [7], we did not see alterations in *ex vivo* MOG34-56 stimulated T cells.

In conclusion, we report that a beneficial effect of CD127 blockade in murine models could not be fully replicated in a marmoset EAE model. It is pertinent to emphasize here that most mouse EAE studies in which efficacy of CD127 blockade was demonstrated were based on MOG-immunized C57BL/6 mice. This frequently used strain is selected for its strong reactivity against MOG. The observation of a positive clinical response to CD127 blockade in high responder marmoset twins implies that the mouse EAE data are essentially replicated in the marmoset EAE model. The reported data therefore does not preclude a potential effect of the anti-CD127 mAb in relapsing-remitting MS in patients, but may predict that only a sub-group of patients may respond.

Acknowledgement

The authors like to thank H. van Westbroek (BPRC) for the artwork and Dr. E. Remarque (BPRC) for statistical advice. J. Dunham was funded by the European Union with a Marie Curie Fellowship (ITN NeuroKine; 316722), and the authors are grateful for this support.

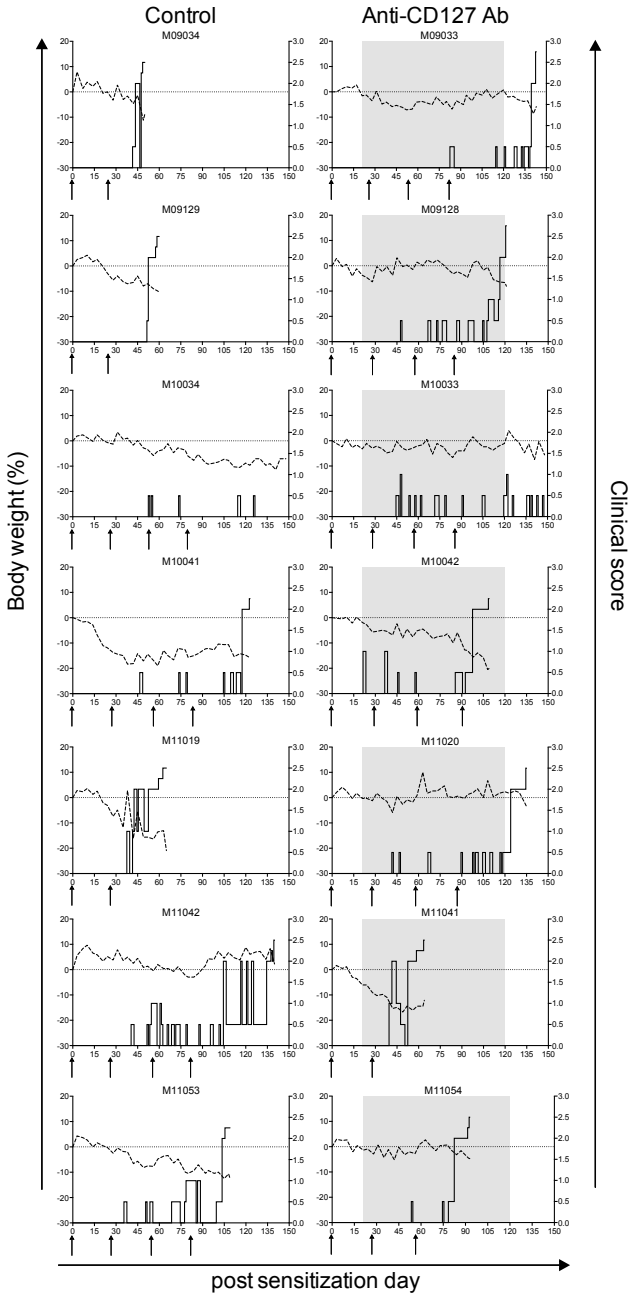

Figure S1. Clinical data. Clinical scores of individual animals. Body weight loss is indicated with a dotted line (left y-axis) and clinical score with a solid line (right y-axis). Treatment period is indicated in grey. Arrows indicate the day of immunization or boost with MOG34-56/IFA.

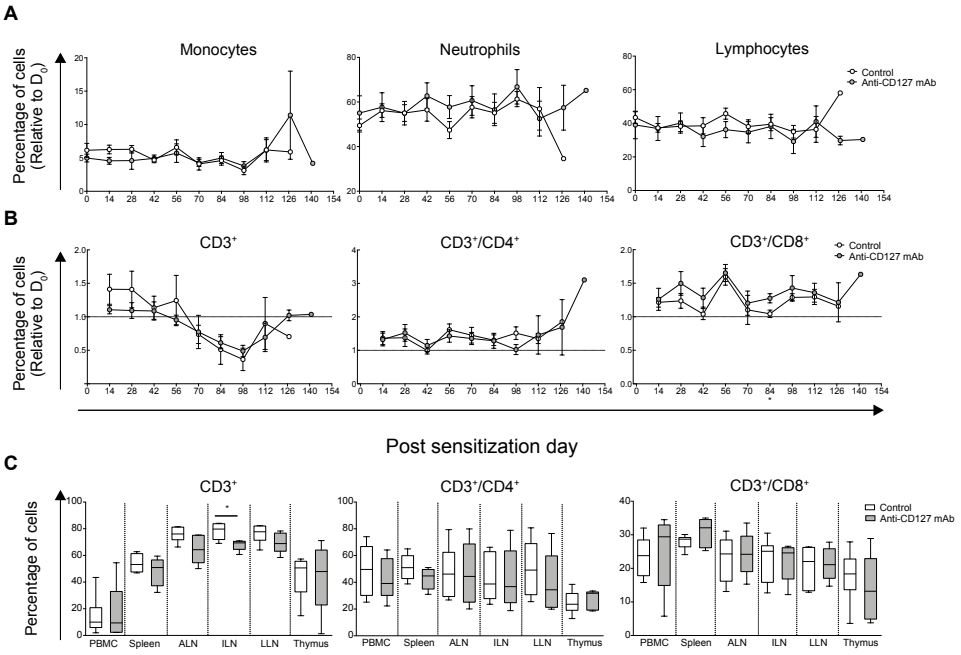

Figure S2. Hematological analysis. A, Hematological analysis during the study showed no treatment-induced alterations of monocytes, neutrophils or lymphocytes populations as a percentage of total white blood cells (n=6). **B**, Isolated PBMC (n=6) during the biweekly bleedings were stained with lymphocyte identification markers and gated based on living cells. No change in percentages CD3+, CD3+CD4+ and CD3+CD8+ T cells isolated from blood were found during the course of the study. **C**, T cell subsets of isolated MNC from SLO and peripheral blood from control (n=6) and treatment (n=5) marmosets.

References

1 Namen, A. E. *et al.* Stimulation of B-cell progenitors by cloned murine interleukin-7. *Nature* **333**, 571-573, doi:10.1038/333571a0 (1988).

2 Lee, L. F. *et al.* IL-7 promotes T(H)1 development and serum IL-7 predicts clinical response to interferon-beta in multiple sclerosis. *Sci Transl Med* **3**, 93ra68, doi:10.1126/scitranslmed.3002400 (2011).

3 Ashbaugh, J. J. *et al.* IL7Ralpha contributes to experimental autoimmune encephalomyelitis through altered T cell responses and nonhematopoietic cell lineages. *J Immunol* **190**, 4525-4534, doi:10.4049/jimmunol.1203214 (2013).

4 Walline, C. C., Kanakasabi, S. & Bright, J. J. IL-7α confers susceptibility to experimental autoimmune encephalomyelitis. *Genes Immun* **12**, 1-14 (2011).

5 Mackall, C. L., Fry, T. J. & Gress, R. E. Harnessing the biology of IL-7 for therapeutic application. *Nat Rev Immunol* **11**, 330-342, doi:10.1038/nri2970 (2011).

6 Kaech, S. M. *et al.* Selective expression of the interleukin 7 receptor identifies effector CD8 T cells that give rise to long-lived memory cells. *Nat Immunol* **4**, 1191-1198, doi:10.1038/ni1009 (2003).

7 Bielekova, B. *et al.* Preferential expansion of autoreactive T lymphocytes from the memory T-cell pool by IL-7. *J Neuroimmunol* **100**, 115-123 (1999).

8 Yilmaz, M., Kendirli, S. G., Altintas, D., Bingol, G. & Antmen, B. Cytokine levels in serum of patients with juvenile rheumatoid arthritis. *Clin Rheumatol* **20**, 30-35 (2001).

9 Bonifati, C. *et al.* Increased interleukin-7 concentrations in lesional skin and in the sera of patients with plaque-type psoriasis. *Clin Immunol Immunopathol* **83**, 41-44 (1997).

10 Jagessar, S. A. *et al.* Induction of progressive demyelinating autoimmune encephalomyelitis in common marmoset monkeys using MOG34-56 peptide in incomplete freund adjuvant. *J Neuropathol Exp Neurol* **69**, 372-385, doi:10.1097/NEN.0b013e3181d5d053 (2010).

11 Kap, Y. S. *et al.* Late B cell depletion with a human anti-human CD20 IgG1kappa monoclonal antibody halts the development of experimental autoimmune encephalomyelitis in marmosets. *J Immunol* **185**, 3990-4003, doi:10.4049/jimmunol.1001393 (2010).

12 Kap, Y. S., van Driel, N., Laman, J. D., Tak, P. P. & 't Hart, B. A. CD20+ B cell depletion alters T cell homing. *J Immunol* **192**, 4242-4253, doi:10.4049/jimmunol.1303125 (2014).

13 Jagessar, S. A. *et al.* B-cell depletion abrogates T cell-mediated demyelination in an antibody-nondependent common marmoset experimental autoimmune encephalomyelitis model. *J Neuropathol Exp Neurol* **71**, 716-728, doi:10.1097/NEN.0b013e3182622691 (2012).

14 Jagessar, S. A. *et al.* The different clinical effects of anti-BLyS, anti-APRIL and anti-CD20 antibodies point at a critical pathogenic role of gamma-herpesvirus infected B cells in the marmoset EAE model. *J Neuroimmune Pharmacol* **8**, 727-738, doi:10.1007/s11481-013-9448-6 (2013).

15 Benjamin, D. *et al.* B cell IL-7. Human B cell lines constitutively secrete IL-7 and express IL-7 receptors. *J Immunol* **152**, 4749-4757 (1994).

16 Haanstra, K. G. *et al.* Induction of experimental autoimmune encephalomyelitis with recombinant human myelin oligodendrocyte glycoprotein in incomplete Freund's adjuvant in three non-human primate species. *J Neuroimmune Pharmacol* **8**, 1251-1264, doi:10.1007/s11481-013-9487-z (2013).

17 Jagessar, S. A. *et al.* Overview of models, methods, and reagents developed for translational autoimmunity research in the common marmoset (*Callithrix jacchus*). *Exp Anim* **62**, 159-171 (2013).

18 Beillard, E. *et al.* Evaluation of candidate control genes for diagnosis and residual disease detection in leukemic patients using 'real-time' quantitative reverse-transcriptase polymerase chain reaction (RQ-PCR) - a Europe against cancer program. *Leukemia* **17**, 2474-2486, doi:10.1038/sj.leu.2403136 (2003).

19 't Hart, B. A., Gran, B. & Weissert, R. EAE: imperfect but useful models of multiple sclerosis. *Trends Mol Med* **17**, 119-125 (2011).

20 Lundmark, F. *et al.* Variation in interleukin 7 receptor alpha chain (IL7R) influences risk of multiple sclerosis. *Nat Genet* **39**, 1108-1113, doi:10.1038/ng2106 (2007).

21 Kreft, K. L. *et al.* The IL-7Ralpha pathway is quantitatively and functionally altered in CD8 T cells in multiple sclerosis. *J Immunol* **188**, 1874-1883, doi:10.4049/jimmunol.1102559 (2012).